Experimental evolution reveals bifunctional genetic solutions to loss of *trpF* in *Salmonella enterica*

Joakim Näsvall[1*] and Hind Abdalaal[1]

[1] Dept. of Medical Biochemistry and Microbiology, Uppsala University, Uppsala, Sweden
[*] Corresponding author. Email: joakim.nasvall@imbim.uu.se

Abstract

How new gene functions arise while maintaining ancestral biological roles remains a central question in evolutionary genetics. To investigate genetic solutions to disruption of a biosynthetic pathway without prior genetic bias, we used experimental evolution to study restoration of tryptophan biosynthesis in *Salmonella enterica* strains lacking the *trpF* gene. Populations were founded from bacteria carrying wild-type alleles of all relevant genes in their native genomic and regulatory contexts and evolved under conditions selecting for growth without exogenous tryptophan. Across independent populations, mutations in either *hisA* or *trpA* enabled growth of Δ*trpF* strains in the absence of added tryptophan while retaining sufficient ancestral function to support growth under the same conditions. Whole-genome sequencing and genetic reconstruction showed that these mutant alleles were sufficient to confer the growth-rescue phenotype. Duplication of the target gene was detected in only a single population and showed no evidence of functional divergence. Mutational paths differed between genes: *hisA*-based solutions arose primarily in mutator backgrounds and were associated with stronger trade-offs with ancestral function, whereas *trpA*-based solutions were more frequent and often retained native function. Together, these results demonstrate that bifunctional genetic solutions can arise through point mutations in multiple genes during experimental adaptation, illustrating how gene-level multifunctionality can evolve without gene duplication.

Introduction

The evolution of new gene functions often involves mutations that alter existing biological roles, creating trade-offs between ancestral and newly acquired activities (Soskine and Tawfik 2010). Such conflicts can be resolved through gene duplication followed by divergence (Ohno 1970; Bergthorsson et al. 2007; Deng et al. 2010; Näsvall et al. 2012). However, although relatively rare in the literature, some genes in nature perform more than one physiologically relevant function, indicating that multifunctionality can also arise and persist without duplication (Mueller et al. 1998; Barona-Gómez and Hodgson 2003). Understanding how genes acquire additional functions while retaining ancestral roles is therefore central to evolutionary genetics, but direct experimental evidence linking specific genetic changes to such outcomes remains limited (Näsvall et al. 2012; Lundin et al. 2020).

One experimental system that has proven particularly informative for studying the evolution of new gene functions involves the histidine and tryptophan biosynthetic pathways in bacteria. In many bacteria, the enzymes HisA and TrpF catalyze chemically related reactions on structurally similar substrates, and both belong to the same family of $(\alpha\beta)_8$-barrel enzymes, reflecting a shared evolutionary origin (Copley and Bork 2000). Consistent with this relationship, previous work has shown that HisA can acquire TrpF activity through mutation, often accompanied by trade-offs with its native function (Jürgens et al. 2000; Näsvall et al. 2012; Newton et al. 2017; Lundin et al. 2020). In addition, some actinobacterial species lack a dedicated *trpF* gene and instead rely on a single HisA ortholog, PriA, that supports both histidine and tryptophan biosynthesis, demonstrating that physiologically relevant bifunctionality can be maintained in nature (Barona-Gómez and Hodgson 2003; Due et al. 2011; Plach et al. 2016).
Additionally, TrpA, an enzyme that acts later in the tryptophan biosynthetic pathway and is less closely related to TrpF, has also been shown to acquire TrpF activity through directed evolution and rational mutagenesis, indicating that multiple genes can, in principle, provide genetic solutions to loss of *trpF* (Evran et al. 2012). However, most previous experimental studies of TrpF replacement have relied on engineered starting genotypes, altered gene expression, or continuous strong selection, potentially biasing evolutionary outcomes toward particular genes or evolutionary paths (Jürgens et al. 2000; Evran et al. 2012; Näsvall et al. 2012; Lundin et al. 2020). As a result, it remains unclear which genes are most likely to evolve physiologically relevant bifunctionality when selection acts on wild-type genetic backgrounds under minimally manipulated conditions.

To reduce experimental biases that can influence which genetic solutions are observed during adaptation, we designed an experimental evolution framework starting from minimally modified genetic backgrounds. We used *Salmonella enterica* strains lacking trpF but otherwise carrying wild-type alleles of *hisA*, *trpA*, and all other relevant genes in their native genomic locations and under their native regulation. Because deletion of *trpF* prevents growth in the absence of tryptophan, populations were propagated in medium containing a limiting amount of tryptophan, allowing initial growth of the ancestral genotype while selecting for restoration of tryptophan biosynthesis as the nutrient became depleted. This approach differs from previous studies that relied on engineered starting alleles, altered gene expression, genomic contexts prone to amplification, or targeted mutagenesis, all of which can bias evolutionary trajectories toward particular genes or mechanisms (Jürgens et al. 2000; Evran et al. 2012; Näsvall et al. 2012; Lundin et al. 2020).

Using this framework, we followed the early stages of adaptation across replicate populations and identified the genetic changes that enabled growth of Δ*trpF* strains without added tryptophan. Whole-genome sequencing and reconstruction of evolved alleles were then used to determine which mutations were sufficient to confer the growth-rescue phenotype, allowing us to characterize the genetic basis and functional consequences of the adaptations that emerged.

Materials and Methods

Bacterial strains and growth conditions

All bacterial strains used in this study (listed in Table S3) are derivatives of *Salmonella enterica* subsp. *enterica* serovar Typhimurium strain LT2, except for three *Escherichia coli* strains used as PCR templates for amplification of selection cassettes employed in λ Red recombineering. Unless otherwise stated, generalized transduction was performed using phage P22 *HT105/1 int-201* (Schmieger 1972) or the defective P22-derived artificial gene transfer agent GTA22 described in the Supplementary Methods.

Lysogeny broth (LB; 10 g/L tryptone, 5 g/L yeast extract, 10 g/L NaCl) was used as rich medium, with 15 g/L Bacto agar added for solid medium (LA). Salt-free LB (LB without NaCl) was used for preparing electrocompetent cells. SOC medium (Hanahan 1983) was used for recovery following electroporation. As minimal medium, M9 medium (Miller 1992) was prepared at double strength with respect to M9 salts, glucose, $CaCl_2$, and $MgCl_2$ (hereafter referred to as 2× M9) to allow growth to higher cell densities. Where indicated, minimal medium was supplemented with tryptophan (0.1 mM or 5 µM), histidine (0.1 mM), and/or guanosine (0.3 mM). Solid M9 plates contained 15 g/L Bacto agar. All cultures were grown at 37 °C except during λ Red recombineering.
Antibiotics were used only for selection of recombinants following genetic manipulations and included trimethoprim (10 mg/L), tetracycline (7.5 mg/L), and chloramphenicol (12.5 mg/L).

PCR and Sanger sequencing

PCR products for λ Red recombineering and Sanger sequencing were generated using Phusion DNA polymerase (Thermo Fisher). PCR templates consisted of bacterial cell suspensions prepared either from a portion of a single colony or from ~1 µL of frozen stock culture resuspended in 100 µL ultrapure water. One microliter of suspension was used per 20 µL PCR reaction. Cycling conditions have been described previously (Näsvall et al. 2017; Näsvall 2017; Näsvall 2022).
PCR products were purified and concentrated by polyethylene glycol (PEG) precipitation using a 2× solution containing 24% (w/v) PEG 8000 and 20 mM $MgCl_2$. DNA pellets were washed with 70% ethanol, air-dried, and resuspended in ultrapure water. For Sanger sequencing, purified PCR products were mixed with sequencing primers (Table S4) and submitted to Eurofins Genomics (Ebersberg, Germany).

λ Red recombineering and genetic reconstructions

Genetic markers, deletions, and allelic replacements were constructed using λ Red recombineering as described previously (Yu et al. 2000; Näsvall et al. 2017; Näsvall 2017; Näsvall 2022). Strains carrying the λ Red helper plasmid pSIM5-Tet (Koskiniemi et al. 2011)

were grown overnight at 30 °C in salt-free LB supplemented with 0.2% glucose, diluted 1:100, and induced for recombination by incubation at 42 °C for 15 min. Cells were rendered electrocompetent by washing in ice-cold water or 10% glycerol and electroporated with purified PCR products.

Mutations in *hisA* and *trpA* were reconstructed by PCR amplification of the mutated alleles from evolved populations or clones, followed by replacement of a selectable and counter-selectable cassette (*Atox1*; GenBank MN207489) inserted at the target locus. Selection for loss of the cassette was performed on M9 medium supplemented with rhamnose (0.2%), histidine, and tryptophan. In cases where evolved alleles contained multiple mutations, overlapping PCR fragments derived from mutant and wild-type templates were used to reconstruct specific alleles.

Deletions, insertions, and selected point mutations were constructed using DIRex with half-cassettes derived from *Atox1* and *Atox2* (GenBank MN207490), as described previously (Näsvall 2017; Näsvall 2022). All oligonucleotides are listed in Table S4.

Experimental evolution

Two experimental evolution studies were performed (outlined in Figure 1).

Experiment 1 was initiated from independent cultures of strain DA52864 (Δ*trpF* ΔP_{gal} Δ*galE*::T_{lux}). Following overnight growth in medium containing histidine and tryptophan, cultures were diluted 1:100 into 5 mL tryptophan-limited medium (2× M9 + 5 µM tryptophan) and propagated by serial transfer. Cultures were passaged once every seven days for 20 cycles and subsequently twice weekly for an additional 30 cycles, totaling approximately 430 generations. Samples were frozen at −80 °C in 20% DMSO at multiple time points.

Experiment 2 was initiated from strains DA62207 (Δ*trpF*) and DA64168 (Δ*trpF mutS*), each carrying a defective P22-derived gene transfer agent (see Supplementary Methods: *Construction and use of an artificial Gene Transfer Agent (GTA22)*). Forty-eight populations were passaged weekly by 1:100 dilution in tryptophan-limited medium for 13 cycles. Samples were frozen at −80 °C in 20% glycerol at multiple time points.

Growth assays and fitness measurements

Growth assays were initiated from overnight cultures grown in 2× M9 supplemented with glucose, histidine, and tryptophan. Cultures were diluted 1:1000 into tryptophan-free or tryptophan-limited medium and transferred to Bioscreen C honeycomb plates. Optical density at 600 nm was recorded every 4 min for up to 7 days at 37 °C with continuous shaking.

Growth rates were estimated by fitting OD data from the exponential phase ($OD_{600} \leq 0.18$) to an exponential growth model using GraphPad Prism. Area under the curve (AUC) values were calculated for the first 72 h following blank subtraction to approximate fitness effects. Additional details and considerations including evaporation effects and post-depletion OD fluctuations that can influence AUC estimates are described in the Supplementary Methods.

Whole-genome re-sequencing

Genomic DNA was extracted from evolving populations using MasterPure DNA purification kits (Epicentre). Libraries for MiSeq sequencing (in-house) were prepared using Nextera XT DNA library preparation and indexing kits (Illumina). Some samples were sequenced by BGI

168 (Beijing, China) using DNBseq technology. Reads were processed and analyzed using CLC
169 Genomics Workbench. Variants were identified by mapping reads to a reference genome
170 containing all known ancestral modifications. Copy number estimates for amplified regions
171 were derived from read depth comparisons as described in the Supplementary Methods.
172

173 ## Results

174 **Experimental evolution restores growth of Δ*trpF* strains under intermittent selection**
175 To identify genetic changes that enable growth of *Salmonella enterica* strains lacking *trpF*
176 under minimally biased conditions, we evolved replicate populations under intermittent
177 selection for rescue of tryptophan prototrophy. Because loss of *trpF* prevents growth only
178 after depletion of exogenous tryptophan, cultures were propagated in medium containing a
179 limiting amount of tryptophan. Each growth cycle therefore began with a period during
180 which all cells could grow, followed by a phase in which continued growth depended on
181 genetic changes that restored the ability to synthesize tryptophan (Figure 1).
182
183 Eight populations were evolved for approximately 430 generations. By the end of the
184 experiment, three populations exhibited detectable growth after tryptophan depletion
185 (Figure 2b; Table 1). Whole-genome sequencing (WGS) revealed that two of these
186 populations carried multiple amino acid substitutions in *hisA* (Tables 1 and S1). Both
187 populations also harbored mutations previously shown to increase mutation rates
188 (frameshift mutations in *mutH* and *mutS*, respectively; Table S1) and accumulated numerous
189 additional mutations across the genome. The mutator mutations were present at low
190 frequencies after approximately 100 generations (Table S1), preceding the appearance of
191 *hisA* mutations by roughly 30 generations (Table S2).
192
193 The third population did not carry mutations in any readily identifiable target gene, and the
194 genetic basis of its ability to grow after tryptophan depletion remains unresolved
195 (Supplementary Results and Discussion: *Two populations evolved TrpF-independent growth*
196 *in still unidentified ways*; Table S1).
197

198 **Mutator status influences both mutation frequency and genetic targets**
199 To further assess the role of elevated mutation rates and to explore alternative evolutionary
200 trajectories, a second experiment was performed in which 24 populations carrying a *mutS*
201 mutation (mutators) and 24 populations without such a mutation (non-mutators) were
202 evolved under the same intermittent selection regime for approximately 78 population
203 doublings.
204
205 After this period, 21 mutator populations and 10 non-mutator populations exhibited
206 detectable growth after tryptophan depletion (Figure 3c,d). WGS of a subset of populations,
207 followed by targeted Sanger sequencing of the remaining populations, identified candidate
208 mutations sufficient to confer the growth-rescue phenotype. These mutations were found
209 either in *hisA* (nine mutator populations) or in *trpA* (11 mutator populations and 10 non-
210 mutator populations).
211
212 TrpA from *S. enterica* has previously been shown to support growth of Δ*trpF* strains through
213 directed evolution and rational mutagenesis (Evran et al. 2012), but had not been identified
214 as a target in prior non-directed evolution experiments. Notably, all sequenced non-mutator

populations and six mutator populations shared the same *trpA* mutation: a 7-bp duplication causing a frameshift. For this mutation to be beneficial under the conditions used here, it must give rise to sufficient amounts of functional protein via ribosomal frameshifting that both substitutes for TrpF in vivo and retains sufficient TrpA function to support growth (see Supplementary Results and Discussion: *How can a frameshift mutation in trpA both create a new function and retain the original function?*). One non-mutator population additionally carried a second *trpA* mutation (A67T) in a subpopulation lacking the frameshift mutation. One mutator population did not acquire mutations in either *hisA* or *trpA*, and its mechanism of adaptation remains unexplained (Supplementary Results and Discussion: *Two populations evolved TrpF-independent growth in still unidentified ways*; Table S1).

Together, these results show that rescue of growth in Δ*trpF* strains can occur through mutations in at least two distinct genes, *hisA* and *trpA*, and that mutator mutations are not required for this outcome, although they influence the types and distributions of mutations observed.

Gene duplication is rare and does not lead to detectable functional divergence

In the minimal medium used for the evolution experiments, growth after tryptophan depletion requires that both histidine and tryptophan biosynthesis remain functional. HisA function is required throughout the growth cycle, whereas TrpA function becomes necessary only after depletion of tryptophan. Despite these constraints, only one whole-genome–sequenced population harbored a duplication or amplification of a relevant target gene (*hisA*). This population carried a single *hisA* allele (Q18R A22T; Table S1) that was supported by 100% of reads mapping to the locus, with no evidence for additional divergent *hisA* alleles. Thus, although amplification occurred in this population, there was no detectable evidence that gene copies had begun to diverge into distinct functional roles.

Evolutionary paths involving *hisA* and *trpA* differ in mutational structure

To determine the order of mutation accumulation in populations carrying multiple mutations in *hisA* or *trpA*, clones were isolated from earlier time points and the target genes were sequenced (Table S2). Consistent with previous work showing that single amino acid substitutions in HisA rarely enable growth of Δ*trpF* strains without compromising growth under histidine-limited conditions (Lundin et al. 2020), all evolutionary paths involving *hisA* began with the same mutation (Q18R).

In contrast, *trpA* exhibited greater diversity in initial mutations, suggesting a broader range of mutational paths that can support growth after tryptophan depletion. To isolate the effects of individual mutations from background mutations accumulated during evolution, all identified *hisA* and *trpA* variants from final populations, as well as most intermediate variants, were reconstructed in an otherwise unevolved genetic background. Growth after tryptophan depletion in these reconstructed strains therefore indicates that the evolved alleles were sufficient to confer the growth-rescue phenotype.

Successive mutations improve growth under selection conditions

Growth of reconstructed strains was assessed in the same minimal medium used during the evolution experiments (Figures 3, S1, S2, S3). During these assays, an unexpected phenotype was observed in which *hisA* mutants grew more slowly in the presence of added tryptophan

262 than in its absence unless guanosine was supplied (Supplementary Results and Discussion:
263 *Supplementing the growth medium with tryptophan causes growth defects that can be*
264 *overridden by guanosine*). This effect likely introduced additional selection pressures
265 unrelated to rescue of tryptophan prototrophy during evolution.
266 To assess the effects of *hisA* mutations independent of this phenotype, guanosine was
267 included in the growth medium. Under these conditions, growth after tryptophan depletion
268 depends on maintenance of native HisA and TrpA functions together with the newly
269 acquired ability to substitute for TrpF *in vivo*. All reconstructed *hisA* and *trpA* variants
270 enabled growth after tryptophan depletion (Figures S1–S3). In most reconstructed
271 mutational pathways, each additional mutation resulted in improved growth following
272 tryptophan depletion.
273
274 **Trade-offs with ancestral function differ between *hisA* and *trpA* variants**
275 Prior to tryptophan depletion, all reconstructed *trpA* mutants grew at rates indistinguishable
276 from the ancestral strain, which itself grew similarly to a $TrpF^+$ prototrophic strain (Figures
277 S3 and S4). This is expected because TrpA function is not required when tryptophan is
278 present in the medium.
279
280 In contrast, all reconstructed *hisA* mutants displayed reduced growth rates relative to the
281 ancestral strain, and successive *hisA* mutations further decreased growth (Figures 4a, S1,
282 S2). Although supplementation with guanosine partially restored growth, all *hisA* mutants
283 still grew significantly more slowly than a wild-type *hisA* control (Figure 4a), consistent with
284 a decline in the native HisA function. As shown previously (Newton et al. 2017), this decline
285 likely reflects combined effects on catalytic properties and other factors that influence total
286 enzyme output *in vivo*.
287
288 Because TrpA and TrpF act within the same biosynthetic pathway, growth curves of *trpA*
289 mutants alone cannot distinguish between changes in the two functions. To assess effects
290 on native TrpA-dependent growth, a wild-type *trpF* gene was expressed from a strong
291 constitutive promoter at an unrelated locus in ten reconstructed *trpA* mutants. Under these
292 conditions, six mutants displayed growth indistinguishable from wild-type controls,
293 indicating minimal impairment of TrpA-dependent growth (Figure 4b). Four mutants grew
294 more slowly, consistent with reduced TrpA function.
295
296 To further evaluate TrpA-dependent growth capacity, wild-type *trpA* and *trpB* were co-
297 expressed from the same locus. Expression of TrpAB improved growth after tryptophan
298 depletion but did not restore growth to the same extent as expression of TrpF, indicating
299 that the TrpF-substituting function was more limiting under these conditions (Figure S5).
300 One growth-compromised variant carried the P62fs frameshift mutation, which is expected
301 to yield low levels of functional protein due to reliance on frameshift suppression. Consistent
302 with this, TrpAB complementation had little effect in this background.
303
304 Three *trpA* variants originated from the same evolutionary pathway in which the initial
305 mutation (G61S) enabled growth of Δ*trpF* strains but impaired TrpA-dependent growth, a
306 second mutation (T24S) improved growth after tryptophan depletion without further loss of
307 TrpA function, and a third mutation (P62S) restored TrpA-dependent growth (Figure S5d–f).
308

Summary of Results

Together, these results show that growth of Δ*trpF* strains under intermittent selection can be restored through mutations in multiple genes without gene duplication and divergence. Mutations in *hisA* and *trpA* both supported rescue of tryptophan prototrophy, but differed in their mutational accessibility and in the extent to which ancestral growth-supporting functions were compromised. These findings provide an empirical basis for understanding how gene-level multifunctionality can emerge during adaptation without gene duplication.

Discussion

This study was designed to identify genetic solutions that restore growth of Δ*trpF* bacteria under conditions intended to minimize experimental bias. In contrast to earlier work that used engineered starting alleles, altered expression, amplification-prone loci, or targeted mutagenesis (Jürgens et al. 2000; Evran et al. 2012; Näsvall et al. 2012; Lundin et al. 2020), we initiated evolution from bacteria carrying wild-type alleles of *hisA*, *trpA*, and other relevant genes in their native genomic and regulatory contexts. Populations were propagated in medium containing a limiting amount of tryptophan, producing intermittent selection for rescue of tryptophan prototrophy as tryptophan became depleted each growth cycle. Under these conditions, mutations in either *hisA* or *trpA* repeatedly enabled growth after tryptophan depletion, and reconstruction of evolved alleles showed that these mutations were sufficient to confer the growth-rescue phenotype (Figure 3b–d; Tables 1, S1, S2; Figures S1–S3).

Multiple genes provide genetic solutions to loss of *trpF* under minimally manipulated conditions

A central result is that Δ*trpF* growth rescue emerged via mutations in at least two different genes, *hisA* and *trpA*, across independent populations (Figure 3; Tables 1 and S1). Prior literature provides clear biochemical precedent that both enzymes can acquire TrpF catalytic activity measurable *in vitro* (Jürgens et al. 2000; Evran et al. 2012; Newton et al. 2017). In addition, previous work has shown that some HisA variants can be bifunctional at the protein level, retaining measurable native activity while also catalyzing the TrpF reaction *in vitro* (Jürgens et al. 2000; Newton et al. 2017), and natural HisA orthologs (PriA) can support both histidine and tryptophan biosynthesis *in vivo* (Barona-Gómez and Hodgson 2003; Due et al. 2011; Plach et al. 2016). Consistent with these earlier findings, the mutations identified here repeatedly generated *genes* that support growth in the absence of *trpF* while retaining sufficient ancestral function to support growth under the same conditions.

Importantly, our primary readout is physiological: the ability of reconstructed alleles to support growth after tryptophan depletion in Δ*trpF* strains. Throughout, “function” refers to this in vivo growth support rather than catalytic rate constants or enzyme kinetics. Accordingly, the central conclusions of this study do not depend on the exact biochemical mechanisms underlying growth rescue, but on the genetic and phenotypic observations that specific evolved *hisA* and *trpA* alleles are sufficient to restore growth in the absence of *trpF* while retaining enough ancestral growth-supporting capacity under the same conditions. This framing is aligned with the objectives of the study—mapping genetic changes to adaptive growth phenotypes—and avoids over-interpreting growth-based outcomes as direct measures of catalytic efficiency.

Mutational accessibility and trade-offs differ between *hisA* and *trpA* solutions

Although both genes repeatedly yielded growth-rescuing alleles, the evolutionary paths

differed. In Experiment 1, *hisA* mutations were found only in populations where mutator alleles appeared prior to the first *hisA* mutations (Tables S1, S2), and in Experiment 2, *hisA* solutions again occurred primarily in *mutS* backgrounds (Figure 2c, d; Table S1). This pattern suggests that, under the conditions used here, mutator status increased access to *hisA*-based solutions, either by elevating the overall supply of rare beneficial mutations or by enabling multi-step paths to be sampled on the relevant timescale. Consistent with this, all reconstructed *hisA* mutants showed reduced growth relative to wild-type *hisA* controls even when guanosine was supplied (Figure 4a), indicating a measurable decline in the ancestral growth-supporting function of HisA.

In contrast, *trpA* solutions were common in both mutator and non-mutator backgrounds (Figure 2c,d; Table S1). Several reconstructed *trpA* variants displayed wild-type growth rates when *trpF* was provided in trans (Figure 4b), consistent with little or no reduction in TrpA-function under those conditions. Other *trpA* variants showed reduced growth that could be improved by providing *trpAB* in trans (Figure S5), indicating that impairment of TrpA function contributed to the phenotype for at least some alleles. Together, these results support the view that *hisA*-based solutions more frequently incur detectable trade-offs with ancestral growth support than *trpA*-based solutions in this experimental context.

One striking outcome was the repeated appearance of a 7-bp duplication causing a frameshift in *trpA* in many non-mutator populations (and in several mutator populations) (Table S1). As discussed in the Supplementary Results and Discussion: *How can a frameshift mutation in trpA both create a new function and retain the original function?*, this allele must yield sufficient functional protein through ribosomal frameshifting to support growth. Regardless of the molecular basis, the recurrence of this mutation indicates that it is an accessible and competitive route to Δ*trpF* growth rescue under the conditions used here.

Gene duplication was rare and did not lead to detectable divergence

A second notable difference from prior work is the low prevalence of gene duplication or amplification. Only one population showed amplification of a relevant target gene (*hisA*) (Table S1), and in this population the reads supported a single *hisA* allele without evidence of divergent gene copies. This contrasts with earlier experimental designs that used amplification-prone genomic contexts and constitutive expression, where duplication and subsequent divergence were central features (Näsvall et al. 2012). Several aspects of the present design could contribute to this difference, including native chromosomal context and regulation of the evolving genes, wild-type starting alleles rather than pre-adapted mutants, and a selective regime in which selection for growth rescue occurs only after tryptophan depletion in each cycle.

While we cannot exclude the possibility that transient duplications arose and were lost during evolution, the absence of duplications in the vast majority of end-point populations, coupled with the absence of evidence for divergent alleles in the single amplified population, indicates that duplication was not a dominant route to adaptation in these experiments. This is consistent with the broader expectation that many duplications carry fitness costs and are genetically unstable, requiring sustained positive selection to be maintained (Hill et al. 1969; Haack and Roth 1995; Reams et al. 2010). Under intermittent selection, any benefit of duplication that is restricted to the post-depletion phase could be reduced by loss during

phases lacking selection for growth rescue, potentially favoring point-mutation routes that produce single genes capable of supporting both requirements.

Intermittent selection creates a stringent and time-dependent filter on adaptive solutions

Growth under the evolution regime reflects more than the ability to resume growth after tryptophan depletion. Even slow-growing or non-growing cells continue to consume resources after depletion of tryptophan, making the time available for additional growth constrained by depletion of other limiting resources. Consequently, a growth-rescue mutation must enable sufficient post-depletion growth to compensate for any pre-depletion deficit and to outcompete other genotypes before the medium becomes exhausted. This time-dependent filter may limit the set of mutations that are not only beneficial in principle but also competitively successful under the specific cycle structure.

More generally, fluctuating selection is known to promote generalist phenotypes at the organismal level, particularly when adaptation involves trade-offs across environments (Kassen 2002; Legros and Koella 2010; Hall et al. 2013; Arribas et al. 2014; Kortright et al. 2022; Fasanello et al. 2024). The present results are consistent with the idea that a similar logic can apply at the gene level: when selection alternates between phases emphasizing different requirements, evolution may favor alleles that satisfy multiple requirements simultaneously, even if those alleles are not optimal for either requirement alone. The cycle structure and frequency of environmental switching are known to influence these outcomes (Roth and Maisnier-Patin 2016; Van Hofwegen et al. 2016), and in this system the alternation between growth with exogenous tryptophan and growth without it provides a clear, repeated switch in selection pressures.

Caveats and interpretation of "bifunctionality" at the gene level

A key point of framing is that our conclusions are based on gene-level phenotypes. The reconstructed *hisA* and *trpA* alleles were sufficient to confer growth after tryptophan depletion in Δ*trpF* strains, while still permitting growth under conditions requiring the ancestral functions (Figures 4, S1–S3). This establishes bifunctionality at the level of *genes supporting two physiological requirements*. It does not, by itself, quantify catalytic activities or identify the biochemical mechanism.

That said, several lines of evidence support the interpretation that the most parsimonious explanation is acquisition of TrpF-like catalytic activity by the mutant proteins while retaining native catalytic function, consistent with prior literature (See Figure S7 for the reactions catalyzed by the three enzymes). First, HisA and TrpA variants that rescue Δ*trpF* in other studies have been shown to possess TrpF catalytic activity *in vitro* (Jürgens et al. 2000; Evran et al. 2012; Newton et al. 2017). Second, some HisA variants with TrpF catalytic activity retain measurable native activity *in vitro* (Jürgens et al. 2000; Newton et al. 2017). Third, in the present study, most *trpA* variants displayed wild-type growth when complemented with *trpF* (Figure 4b), supporting retention of TrpA function *in vivo* for many alleles. Conversely, where complementation experiments indicated partial deficits, they are consistent with altered TrpA function rather than bypass of the pathway (Figure S5). For a speculative discussion on potential mechanisms of action of the evolved HisA and TrpA proteins, see Supplementary Results and Discussion: *Speculative considerations for ΔtrpF rescue by evolved HisA and TrpA proteins* and Figure S8. While alternative mechanisms

cannot be formally excluded, the combination of genetic sufficiency and the strong precedent for enzymatic acquisition in this system supports the interpretation that the mutant proteins are capable of catalyzing both their native reactions and that they can substitute for the missing TrpF.

Conclusions

By evolving Δ*trpF* populations under a selective regime designed to reduce experimental bias, we found that point mutations in multiple genes (*hisA* and *trpA*) can repeatedly rescue growth without exogenous tryptophan while retaining sufficient ancestral growth-supporting functions. Mutational paths and trade-offs differed between genes, and gene duplication was rare and showed no evidence of divergence. Together with prior biochemical and comparative evidence (Jürgens et al. 2000; Barona-Gómez and Hodgson 2003; Due et al. 2011; Evran et al. 2012; Plach et al. 2016; Newton et al. 2017), these results support the broader conclusion that gene-level multifunctionality can emerge during adaptation without gene duplication, and that the structure of selection—here, intermittent selection imposed by nutrient depletion—can shape which genetic solutions are accessible and successful.

Data availability

All genome re-sequencing data have been deposited in the Sequence Read Archive (SRA) with BioProject accession code PRJNA1092712.

Acknowledgements

We thank Anna Knöppel, Omar Warsi, Ramith Nair, and Dan Andersson for critical reading of the manuscript.

Funding

This work was founded by the Swedish Research Council (VR-NT 2020-03512) and the Carl Trygger Foundation (CTS 22:2094).

Author Contributions

JN conceived the study, constructed bacterial strains, made bacterial growth rate assays and analyzed data. HA and JN performed evolution experiments, and isolated and sequenced clones from evolved populations. HA wrote an early draft of the manuscript as part of her PhD thesis, JN re-worked and extended the manuscript.

Competing interests

None.

Supplementary Information

Supplementary Information is available for this paper.

Correspondence

Correspondence and requests for materials should be addressed to JN.

497 **References**

498 Arribas M, Kubota K, Cabanillas L, Lázaro E. 2014. Adaptation to Fluctuating Temperatures in an RNA Virus Is
499 Driven by the Most Stringent Selective Pressure. PLOS ONE. 9(6):e100940.
500 https://doi.org/10.1371/journal.pone.0100940

501 Barona-Gómez F, Hodgson DA. 2003. Occurrence of a putative ancient-like isomerase involved in histidine and
502 tryptophan biosynthesis. EMBO Rep. 4(3):296–300. https://doi.org/10.1038/sj.embor.embor771

503 Bergthorsson U, Andersson DI, Roth JR. 2007. Ohno's dilemma: Evolution of new genes under continuous
504 selection. Proc Natl Acad Sci. 104(43):17004–17009. https://doi.org/10.1073/pnas.0707158104

505 Copley RR, Bork P. 2000. Homology among (βα)8 barrels: implications for the evolution of metabolic
506 pathways1. J Mol Biol. 303(4):627–641. https://doi.org/10.1006/jmbi.2000.4152

507 Deng C et al. 2010. Evolution of an antifreeze protein by neofunctionalization under escape from adaptive
508 conflict. Proc Natl Acad Sci. 107(50):21593–21598. https://doi.org/10.1073/pnas.1007883107

509 Due AV et al. 2011. Bisubstrate specificity in histidine/tryptophan biosynthesis isomerase from Mycobacterium
510 tuberculosis by active site metamorphosis. Proc Natl Acad Sci U S A. 108(9):3554–3559.
511 https://doi.org/10.1073/pnas.1015996108

512 Evran S, Telefoncu A, Sterner R. 2012. Directed evolution of (βα)8-barrel enzymes: establishing
513 phosphoribosylanthranilate isomerisation activity on the scaffold of the tryptophan synthase α-subunit. Protein
514 Eng Des Sel. 25(6):285–293. https://doi.org/10.1093/protein/gzs015

515 Fasanello VJ, Liu P, Fay JC, Botero CA. 2024. Fluctuating selection facilitates the discovery of broadly effective
516 but difficult to reach adaptive outcomes in yeast. Evol Lett. 8(2):243–252.
517 https://doi.org/10.1093/evlett/qrad055

518 Haack KR, Roth JR. 1995. Recombination between chromosomal IS200 elements supports frequent duplication
519 formation in Salmonella typhimurium. Genetics. 141(4):1245–1252.
520 https://doi.org/10.1093/genetics/141.4.1245

521 Hall JP, Harrison E, Brockhurst MA. 2013. Viral host-adaptation: insights from evolution experiments with
522 phages. Curr Opin Virol. 3(5):572–577 (Antivirals and resistance / Virus evolution).
523 https://doi.org/10.1016/j.coviro.2013.07.001

524 Hanahan D. 1983. Studies on transformation of Escherichia coli with plasmids. J Mol Biol. 166(4):557–580.
525 https://doi.org/10.1016/S0022-2836(83)80284-8

526 Hill CW, Foulds J, Soll L, Berg P. 1969. Instability of a missense suppressor resulting from a duplication of
527 genetic material. J Mol Biol. 39(3):563–581. https://doi.org/10.1016/0022-2836(69)90146-6

528 Jürgens C et al. 2000. Directed evolution of a (beta alpha)8-barrel enzyme to catalyze related reactions in two
529 different metabolic pathways. Proc Natl Acad Sci U S A. 97(18):9925–9930.
530 https://doi.org/10.1073/pnas.160255397

531 Kassen R. 2002. The experimental evolution of specialists, generalists, and the maintenance of diversity. J Evol
532 Biol. 15(2):173–190. https://doi.org/10.1046/j.1420-9101.2002.00377.x

533 Kortright KE, Chan BK, Evans BR, Turner PE. 2022. Arms race and fluctuating selection dynamics in
534 Pseudomonas aeruginosa bacteria coevolving with phage OMKO1. J Evol Biol. 35(11):1475–1487.
535 https://doi.org/10.1111/jeb.14095

536 Koskiniemi S et al. 2011. Activation of cryptic aminoglycoside resistance in Salmonella enterica. Mol Microbiol.
537 80(6):1464–1478. https://doi.org/10.1111/j.1365-2958.2011.07657.x

538 Legros M, Koella JC. 2010. Experimental evolution of specialization by a microsporidian parasite. BMC Evol Biol.
539 10(1):159. https://doi.org/10.1186/1471-2148-10-159

540 Lundin E, Näsvall J, Andersson DI. 2020. Mutational Pathways and Trade-Offs Between HisA and TrpF Functions:
541 Implications for Evolution via Gene Duplication and Divergence. Front Microbiol. 11:588235.
542 https://doi.org/10.3389/fmicb.2020.588235

543 Miller JH. 1992. A short course in bacterial genetics: a laboratory manual and handbook for Escherichia coli and
544 related bacteria. Cold Spring Harbor Laboratory Press.

545 Mueller EG et al. 1998. Identification of a gene involved in the generation of 4-thiouridine in tRNA. Nucleic
546 Acids Res. 26(11):2606–2610. https://doi.org/10.1093/nar/26.11.2606

547 Näsvall J. 2017. Direct and Inverted Repeat stimulated excision (DIRex): Simple, single-step, and scar-free
548 mutagenesis of bacterial genes. PloS One. 12(8):e0184126. https://doi.org/10.1371/journal.pone.0184126

549 Näsvall J. 2022. Dup-In and DIRex: Techniques for Single-Step, Scar-Free Mutagenesis with Marker Recycling. In:
550 Reisch CR, editor. Recombineering: Methods and Protocols. Springer US; p 85–104 (Methods in Molecular
551 Biology). [accessed 2022 May 23]. https://doi.org/10.1007/978-1-0716-2233-9_7. https://doi.org/10.1007/978-
552 1-0716-2233-9_7

553 Näsvall J, Knöppel A, Andersson DI. 2017. Duplication-Insertion Recombineering: a fast and scar-free method
554 for efficient transfer of multiple mutations in bacteria. Nucleic Acids Res. 45(5):e33.
555 https://doi.org/10.1093/nar/gkw1078

556 Näsvall J, Sun L, Roth JR, Andersson DI. 2012. Real-time evolution of new genes by innovation, amplification,
557 and divergence. Science. 338(6105):384–387. https://doi.org/10.1126/science.1226521

558 Newton MS et al. 2017. Structural and functional innovations in the real-time evolution of new (βα)8 barrel
559 enzymes. Proc Natl Acad Sci U S A. 114(18):4727–4732. https://doi.org/10.1073/pnas.1618552114

560 Ohno S. 1970. Evolution by Gene Duplication. Springer-Verlag. http://link.springer.com/10.1007/978-3-642-
561 86659-3. https://doi.org/10.1007/978-3-642-86659-3

562 Plach MG, Reisinger B, Sterner R, Merkl R. 2016. Long-Term Persistence of Bi-functionality Contributes to the
563 Robustness of Microbial Life through Exaptation. PLOS Genet. 12(1):e1005836.
564 https://doi.org/10.1371/journal.pgen.1005836

565 Reams AB, Kofoid E, Savageau M, Roth JR. 2010. Duplication Frequency in a Population of Salmonella enterica
566 Rapidly Approaches Steady State With or Without Recombination. Genetics. 184(4):1077–1094.
567 https://doi.org/10.1534/genetics.109.111963

568 Roth JR, Maisnier-Patin S. 2016. Reinterpreting Long-Term Evolution Experiments: Is Delayed Adaptation an
569 Example of Historical Contingency or a Consequence of Intermittent Selection? J Bacteriol. 198(7):1009–1012.
570 https://doi.org/10.1128/jb.00110-16

571 Schmieger H. 1972. Phage P22-mutants with increased or decreased transduction abilities. Mol Gen Genet
572 MGG. 119(1):75–88. https://doi.org/10.1007/BF00270447

573 Soskine M, Tawfik DS. 2010. Mutational effects and the evolution of new protein functions. Nat Rev Genet
574 2015 168. 11(8):572–582. https://doi.org/10.1038/nrg2808

575 Van Hofwegen DJ, Hovde CJ, Minnich SA. 2016. Rapid Evolution of Citrate Utilization by Escherichia coli by
576 Direct Selection Requires citT and dctA. J Bacteriol. 198(7):1022–1034. https://doi.org/10.1128/jb.00831-15

577 Yu D et al. 2000. An efficient recombination system for chromosome engineering in Escherichia coli. Proc Natl
578 Acad Sci U S A. 97(11):5978–5983. https://doi.org/10.1073/pnas.100127597

579

Table 1. Identified mutations conferring TrpF activity.

Strain #	Population[a]	# Generations[b]	Causative mutation(s)[c]	Identified by[d]
DA59062	1-1	430	*hisA*[Q18R A22T R23L K107E V168A]	WGS
DA59064	1-3	430	*hisA*[Q18R A22T V168A]	WGS
DA59068	1-7	430	(not identified)[e]	WGS
DA65429	2mut+3	78	*trpA*[P62R(fs)]	WGS
DA65433	2mut+7	78	*trpA*[P62R(fs)]	WGS
DA65434	2mut+8	78	*trpA*[P62R(fs)]	WGS
DA65435	2mut+9	78	*trpA*[P62R(fs)]	WGS
DA65436	2mut+10	78	*trpA*[P62R(fs)]	WGS
DA65437	2mut+11	78	*trpA*[P62R(fs)]	WGS
DA65438	2mut+12	78	*trpA*[P62R(fs)]	WGS
DA65445	2mut+19	78	*trpA*[P62R(fs)]	WGS
DA65447	2mut+21	78	*trpA*[P62R(fs)], *trpA*[A67T]	WGS
DA65449	2mut+23	78	*trpA*[P62R(fs)]	WGS
DA65451	2mutS1	78	*hisA*[Q18R]	Sanger
DA65452	2mutS2	78	*hisA*[Q18R A127G]	WGS
DA65453	2mutS3	78	*hisA*[Q18R H17R]	WGS
DA65454	2mutS4	78	*trpA*[D27Y G98S]	Sanger
DA65456	2mutS6	78	*trpA*[P62R(fs)]	Sanger
DA65457	2mutS7	78	*trpA*[P62R(fs)]	Sanger
DA65458	2mutS8	78	*hisA*[Q18R A22T] (8-fold amplified)[f]	WGS
DA65459	2mutS9	78	*hisA*[Q18R]	Sanger
DA65460	2mutS10	78	*hisA*[Q18R]	Sanger
DA65461	2mutS11	78	*trpA*[G98C]	Sanger
DA65462	2mutS12	78	*trpA*[P62R(fs)]	WGS
DA65463	2mutS13	78	*trpA*[P62R(fs)]	Sanger
DA65464	2mutS14	78	*trpA*[G98S Y102H Q250R]	Sanger
DA65465	2mutS15	78	*trpA*[P62R(fs)]	Sanger
DA65466	2mutS16	78	*trpA*[T24S G61S P62S]	WGS
DA65467	2mutS17	78	*hisA*[Q18R]	Sanger
DA65468	2mutS18	78	*hisA*[Q18R]	WGS
DA65469	2mutS19	78	*hisA*[Q18R T52S]	Sanger
DA65471	2mutS21	78	*trpA*[P62R(fs)]	Sanger
DA65472	2mutS22	78	(not identified)[e]	WGS
DA65473	2mutS23	78	*trpA*[D27Y G98C]	WGS

[a] Only populations that could grow significantly denser than their ancestor within 7 days at the end of the experiment are listed. The populations are named according to which evolution experiment (1 or 2) they were part of, and the order the cultures were handled in during passages (1 – 8 and 1 – 24, respectively for the first and second evolution experiment). The populations from the second experiment additionally have "mut+" for non-mutators and "mutS" for mutators.

[b] The numbers of generations were calculated from the fold dilution and the number of passages [$\log_2$(dilution)×passages] and reflect the minimum number of generations for the population as a whole.

[c] The mutations listed have been re-constructed in the genetic background of the non-evolved ancestral strain (Δ*trpF*), and has been verified to confer growth in the absence of tryptophan.

[d] Mutations were identified either through whole genome sequencing (WGS) or Sanger sequencing (targeting the *trpA* and *hisA* genes). For a complete list of mutations present at high frequencies in the whole-genome sequenced populations, see Table S1.

[e] These populations did not have any mutations in *hisA* or *trpA*.

[f] This population contained a ~19 kb amplification encompassing the entire *his* operon at ~8-fold coverage compared to the surrounding genomic DNA.

580

Figures

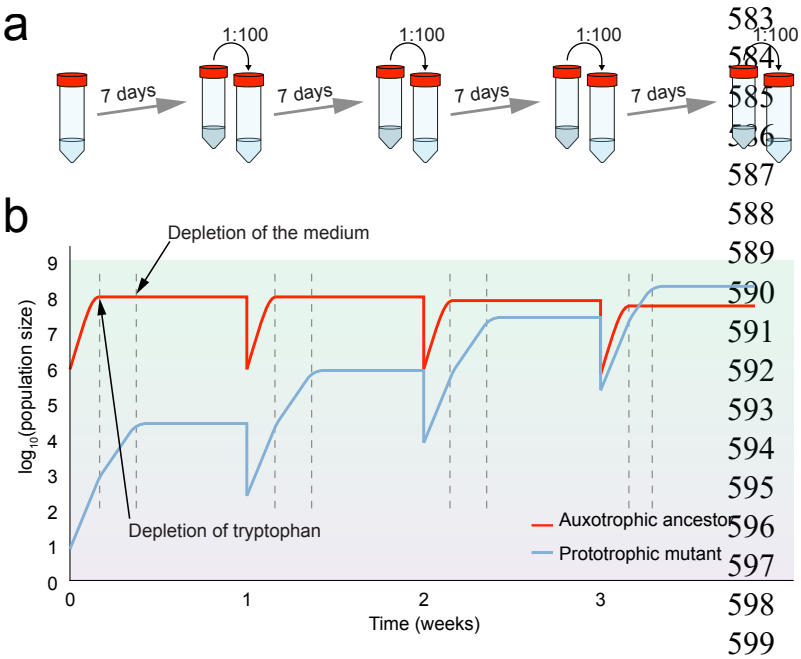

Figure 1. Experimental outline. **(a)** Serial passage experiments with *Salmonella enterica* lacking the *trpF* gene, grown in media with limiting tryptophan. Each 7-day cycle consisted of a short period with unlimited growth (tryptophan present) followed by a longer period without tryptophan (tryptophan-limited selection). Only prototrophic mutants (that had gained TrpF activity) could grow during this phase. **(b)** The expected dynamics during the takeover of a batch culture population by a TrpF+ mutant competing with its TrpF- ancestor in tryptophan-limited medium. Each cycle includes a brief window where the TrpF+ mutant can grow and outcompete the TrpF- ancestor. The TrpF- ancestor is expected to seize growing when tryptophan is depleted while the TrpF+ mutant continues growing until the medium is depleted for some other essential nutrient(s). Initially, the non-growing TrpF- ancestor sets the window by continuing to metabolize and consume resources, thereby limiting the time available for the TrpF+ mutant to grow. However, once the TrpF+ mutant becomes dominant, it will determine the length of the window through its own metabolic activity.

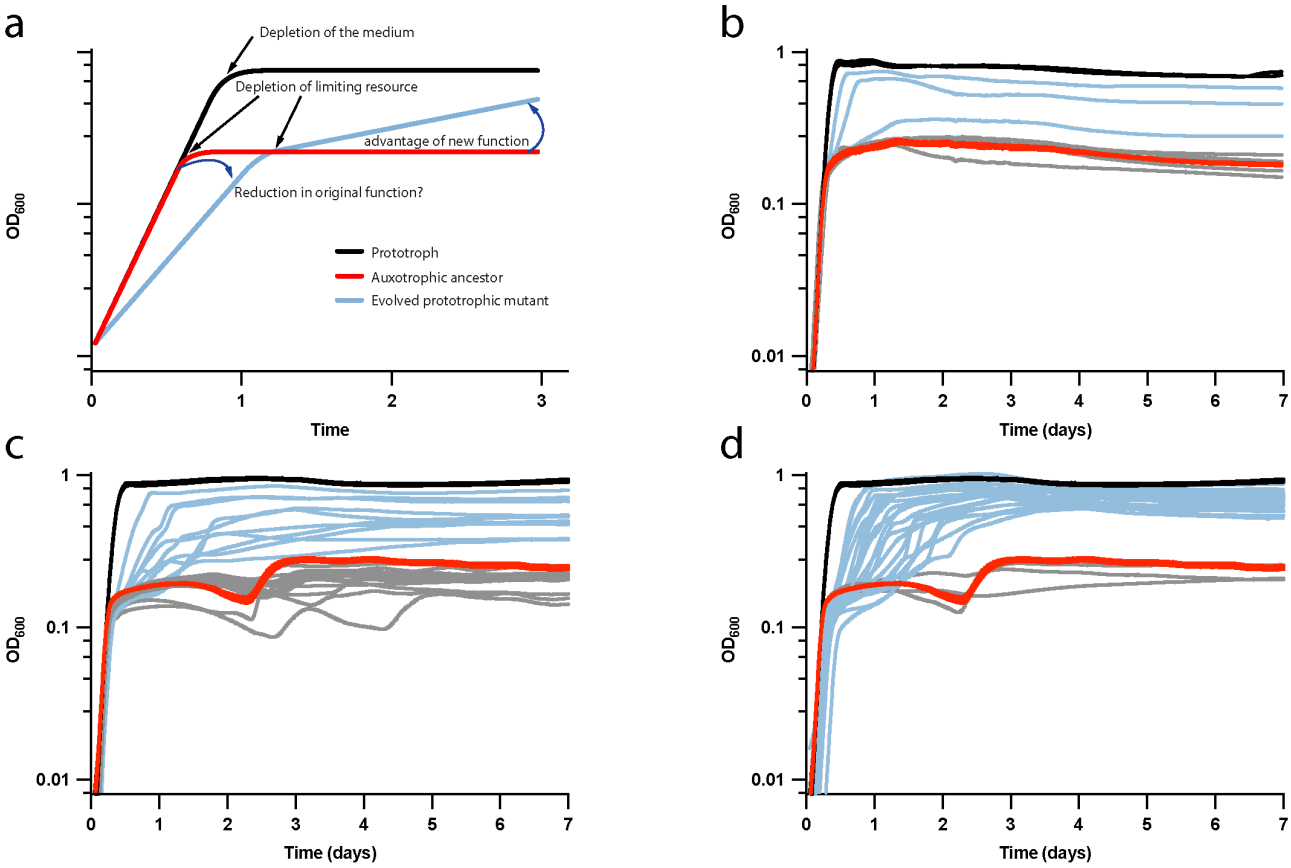

Figure 2. Growth Dynamics of Prototrophic and Auxotrophic Strains under Limiting Resources. **(a)** Hypothetical growth curves: the expected growth behaviour of a prototrophic strain (black), an auxotrophic strain (red), and an evolving prototroph (blue) under limiting resource conditions. The auxotroph (red) is expected to grow until the limiting resource is depleted and enter stationary phase at low population density. The prototroph (black) can continue growing until depletion of other essential nutrients or changes in medium composition (e.g., pH or metabolite accumulation) halt growth. The evolved prototroph (blue) exhibits growth after the limiting resource depletion, with a rate dependent on the rate of its newly acquired activity. If the original enzyme function is crucial for growth, reduced activity due to a mutation might lead to a slower growth rate before the limiting resource is depleted. **(b – d)** Batch growth curves of a tryptophan prototroph (*trpF*+, black), the ancestral tryptophan auxotroph (Δ*trpF*, red), the evolving populations from the final time-point that gained tryptophan independent growth (blue), and those that did not (grey). **(b)** The eight lineages from the first experiment. **(c)** The 24 non-mutator lineages from the second experiment. **(d)** The 24 mutator lineages from the second experiment (compared to the ancestral non-mutator strain).

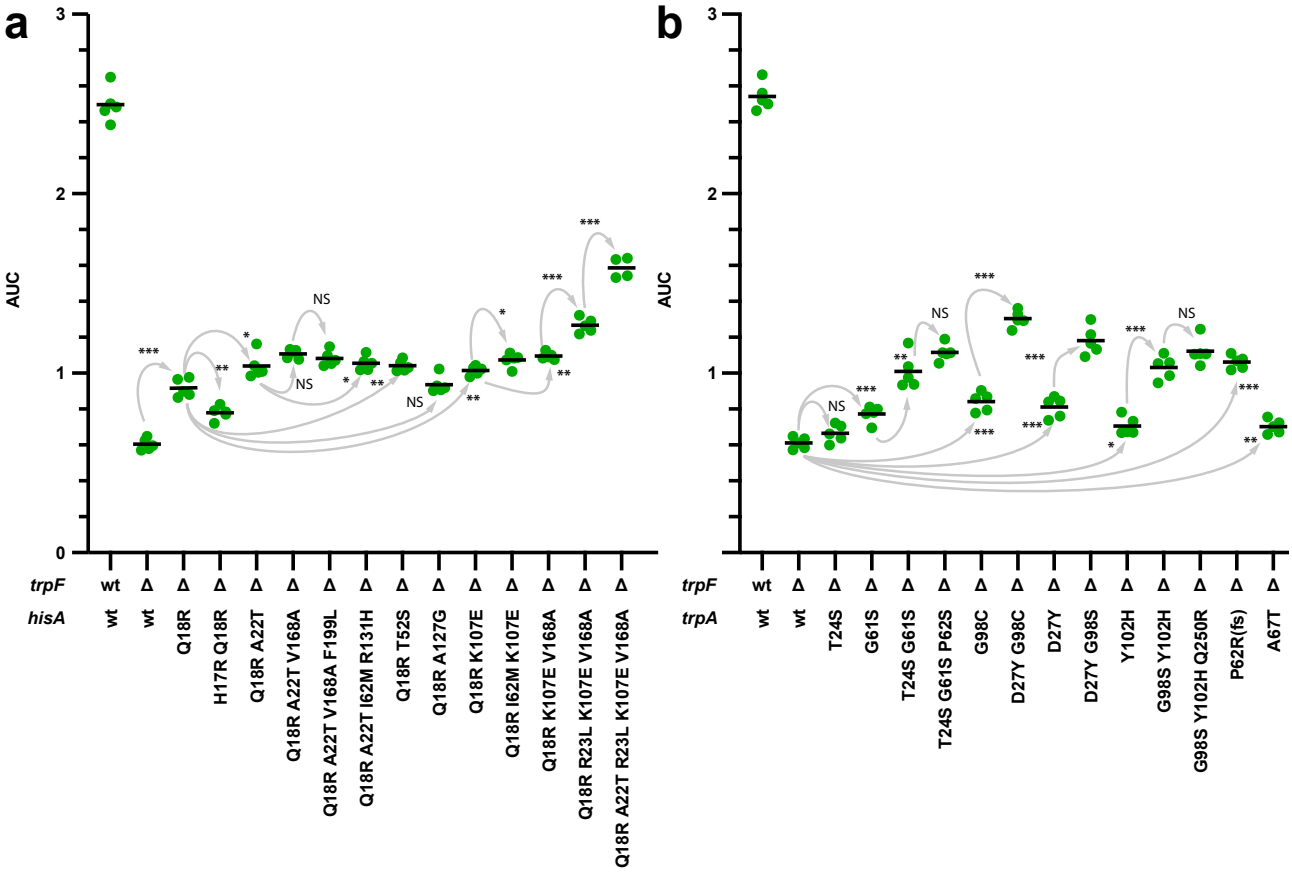

Figure 3. Growth of re-constructed mutants in tryptophan-limited medium. **(a)** *hisA* mutants. **(b)** *trpA* mutants. Reconstructed mutants were grown in M9 glucose minimal medium supplemented with limiting tryptophan (5 µM) and guanosine (3 mM). As growth under these conditions deviates from exponential growth (except for the TrpF+ control strain), growth is reported as the area under the curve (AUC) for the first 3 days (see Methods for details). Black bars represent averages. NS, non-significant ($p > 0.05$); *, $p < 0.05$; **, $p < 0.005$; ***, $p < 0.0005$, based on a two-tailed Student's t-test with equal variance. Only the two rightmost *trpA* mutants were found in non-mutator populations, all others (in both genes) were found in hypermutators. Each mutant was compared to its immediate ancestor, indicated by the grey arrows. All strains were grown in at least four independent biological replicates. The complete growth curves can be found in Figures S1, S2, S3.

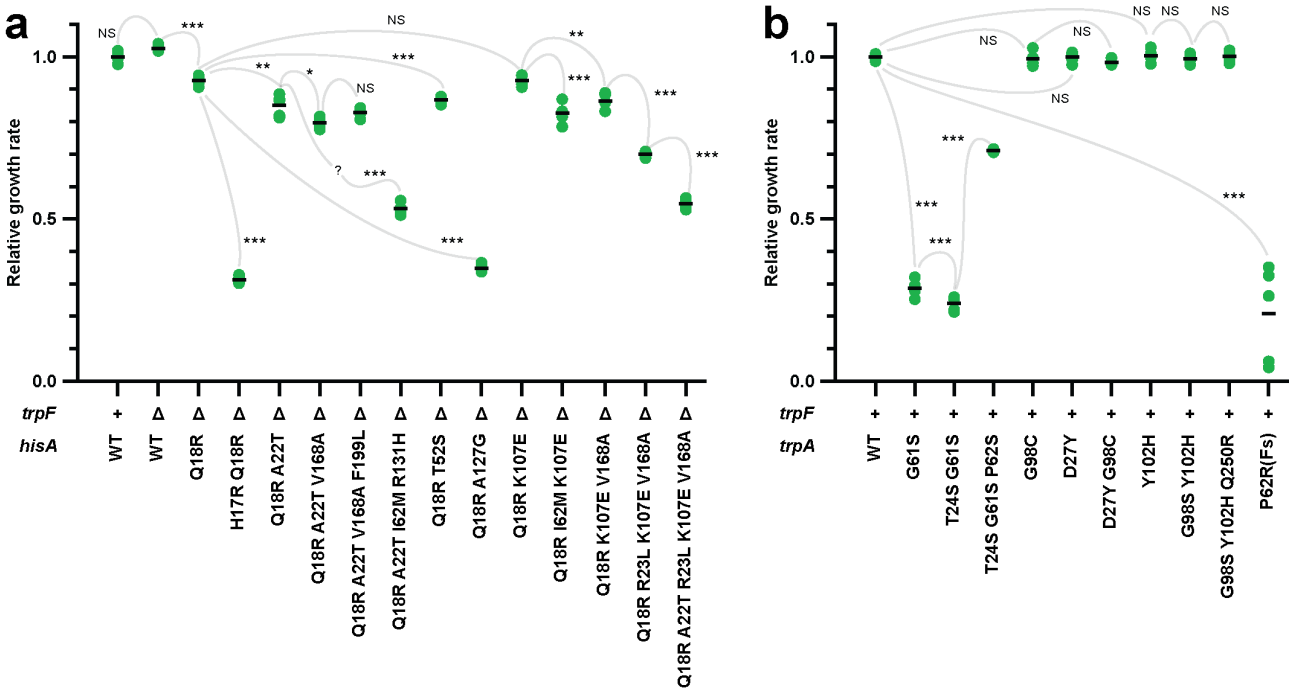

Figure 4. Impact of Mutations on native function. **(a)** HisA function: Exponential growth rates were measured in the early, rapid growth phase ($0.095 < OD_{600} < 0.184$) before tryptophan depletion in M9 glucose medium supplemented with limiting tryptophan (5 µM) and guanosine (3 mM). Rates were normalized to the growth rate of the *trpF*+ wild-type strain grown in the same experiment. Under these conditions, reductions in HisA activity lead to decreased growth rates. Strains were grown in four or five biological replicates. Grey lines connect each mutant to its immediate ancestor. The question mark indicates an unknown mutation order in the evolution experiment, preventing complete reconstruction of the path. **(b)** TrpA function: Exponential growth rates were measured in M9 glucose medium without supplements for strains expressing wild-type *trpF* from a constitutive promoter at a different locus. Here, reductions in TrpA function lead to decreased growth rates. For *trpA* mutants under the same conditions as (a), see Figure S4, and for growth curves of strains complemented with *trpF* or *trpA*, see Figure S5. NS, non-significant (difference in growth rate < 5% or p > 0.05). Asterisks indicate significance levels (*, $p < 0.05$; **, $p < 0.005$; ***, $p < 0.0005$) based on two-tailed Student's *t*-tests with equal variance, comparing each mutant to its immediate ancestor (grey lines).

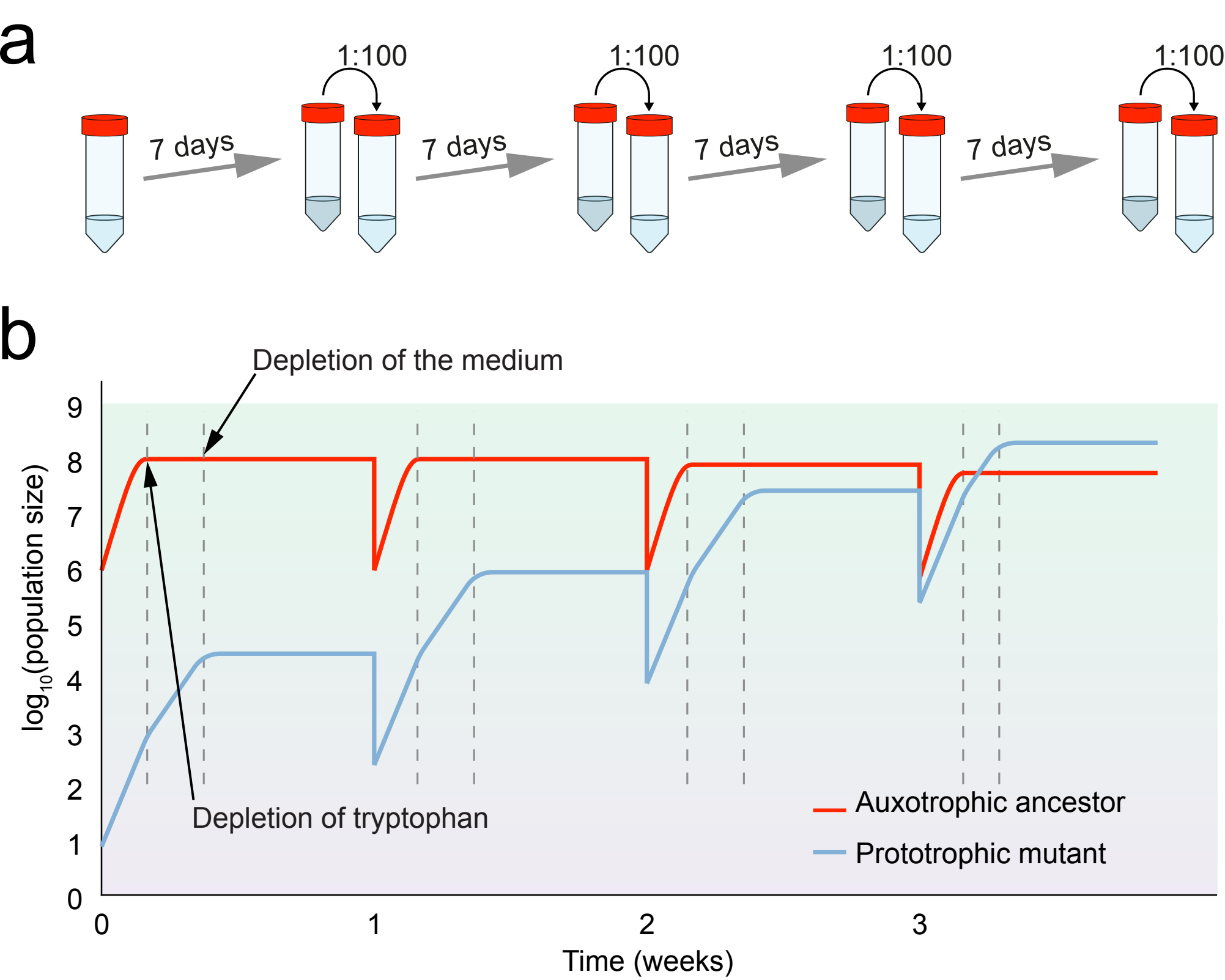
a
1:100
1:100
1:100
1:100
7 days
7 days
7 days
7 days
b
Depletion of the medium
Depletion of tryptophan
Auxotrophic ancestor
Prototrophic mutant
log10(population size)
0
1
2
3
4
5
6
7
8
9
0
1
2
3
Time (weeks)

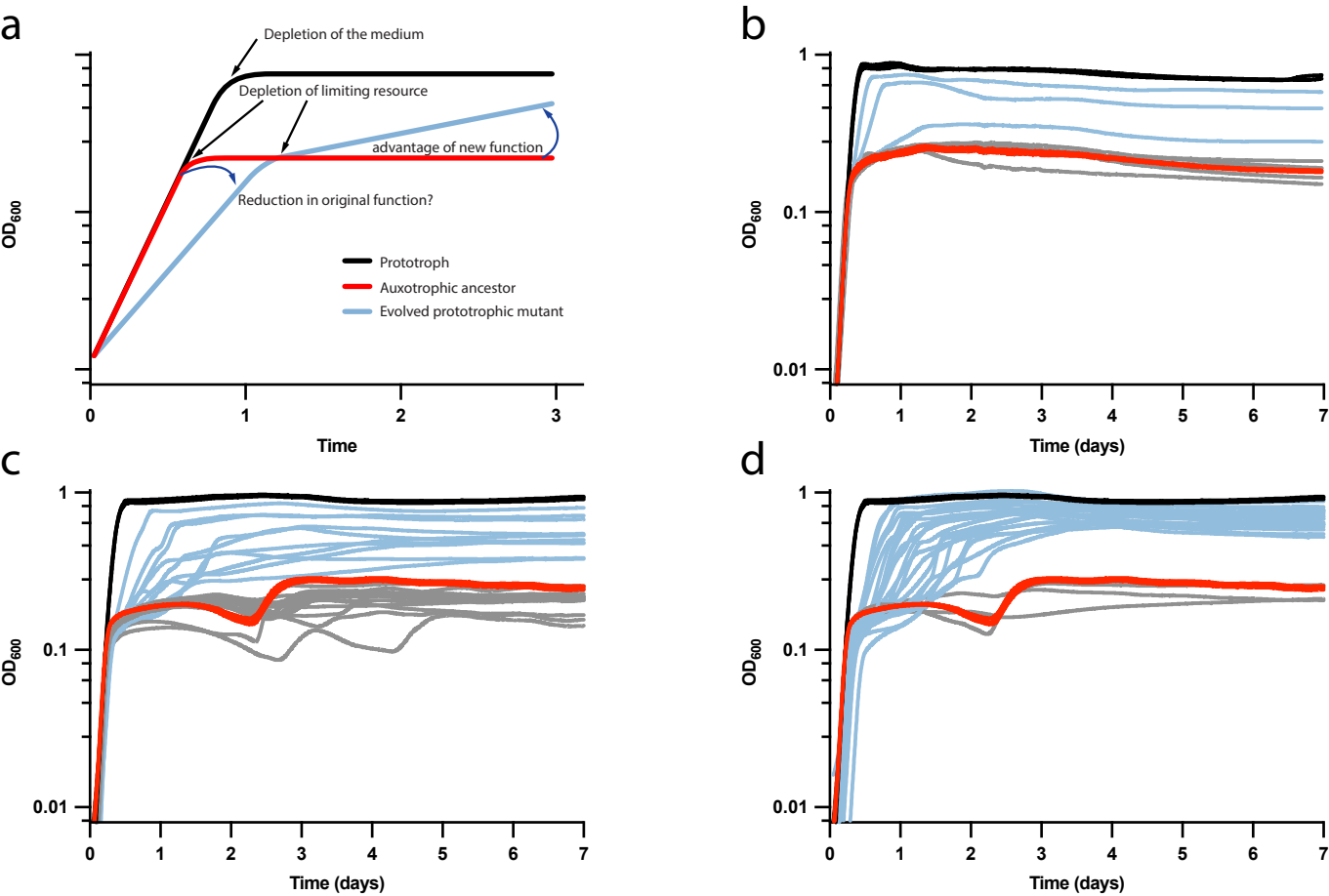
a
Depletion of the medium
Depletion of limiting resource
advantage of new function
Reduction in original function?
Prototroph
Auxotrophic ancestor
Evolved prototrophic mutant
OD600
Time
0
1
2
3
b
c
d
1
0.1
0.01
4
5
6
7
Time (days)

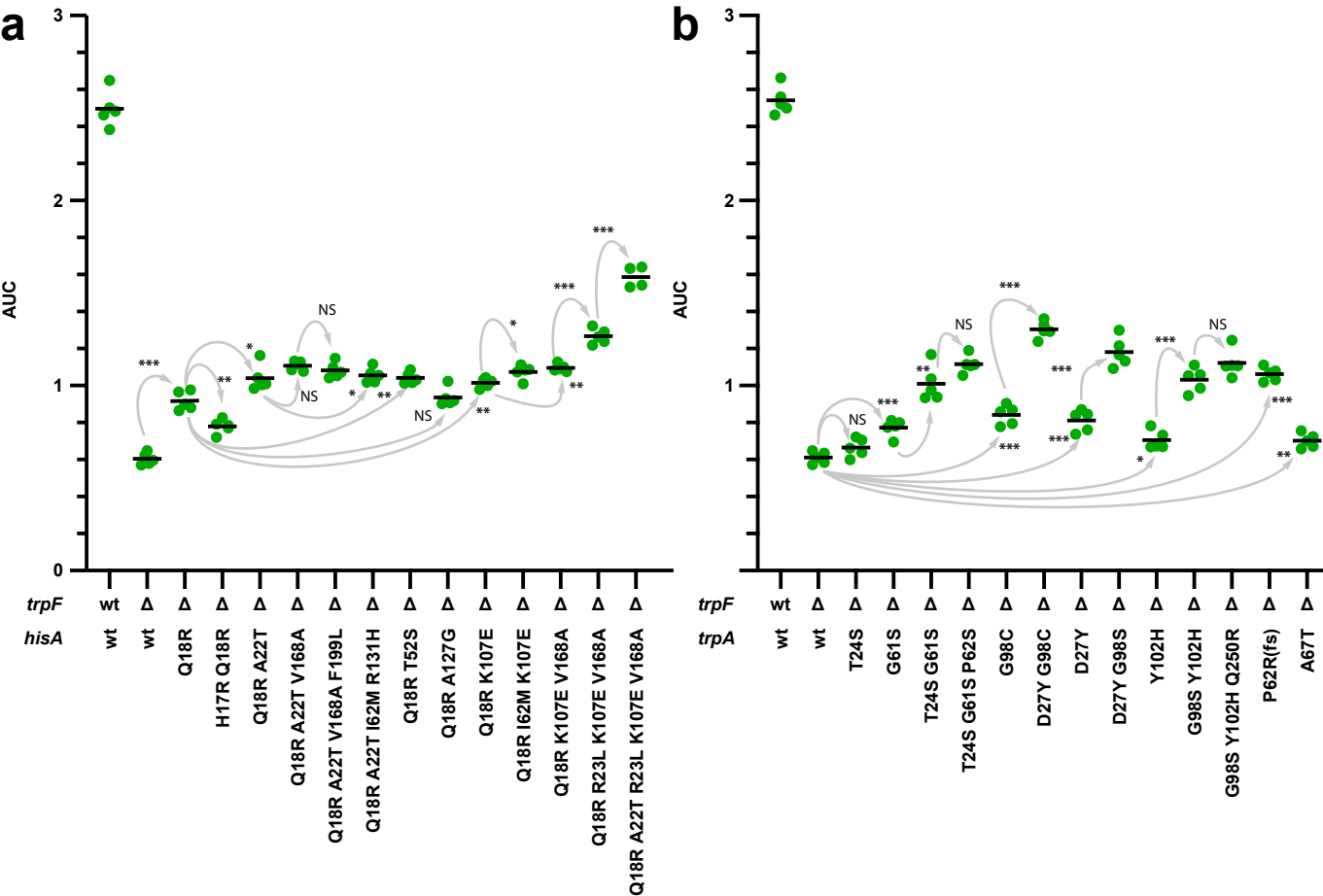
a
b
AUC
0
1
2
3
trpF
hisA
trpA
wt
Δ
Q18R
H17R Q18R
Q18R A22T
Q18R A22T V168A
Q18R A22T V168A F199L
Q18R A22T I62M R131H
Q18R T52S
Q18R A127G
Q18R K107E
Q18R I62M K107E
Q18R K107E V168A
Q18R R23L K107E V168A
Q18R A22T R23L K107E V168A
T24S
G61S
T24S G61S
T24S G61S P62S
G98C
D27Y G98C
D27Y
D27Y G98S
Y102H
G98S Y102H
G98S Y102H Q250R
P62R(fs)
A67T
NS
*
**
***

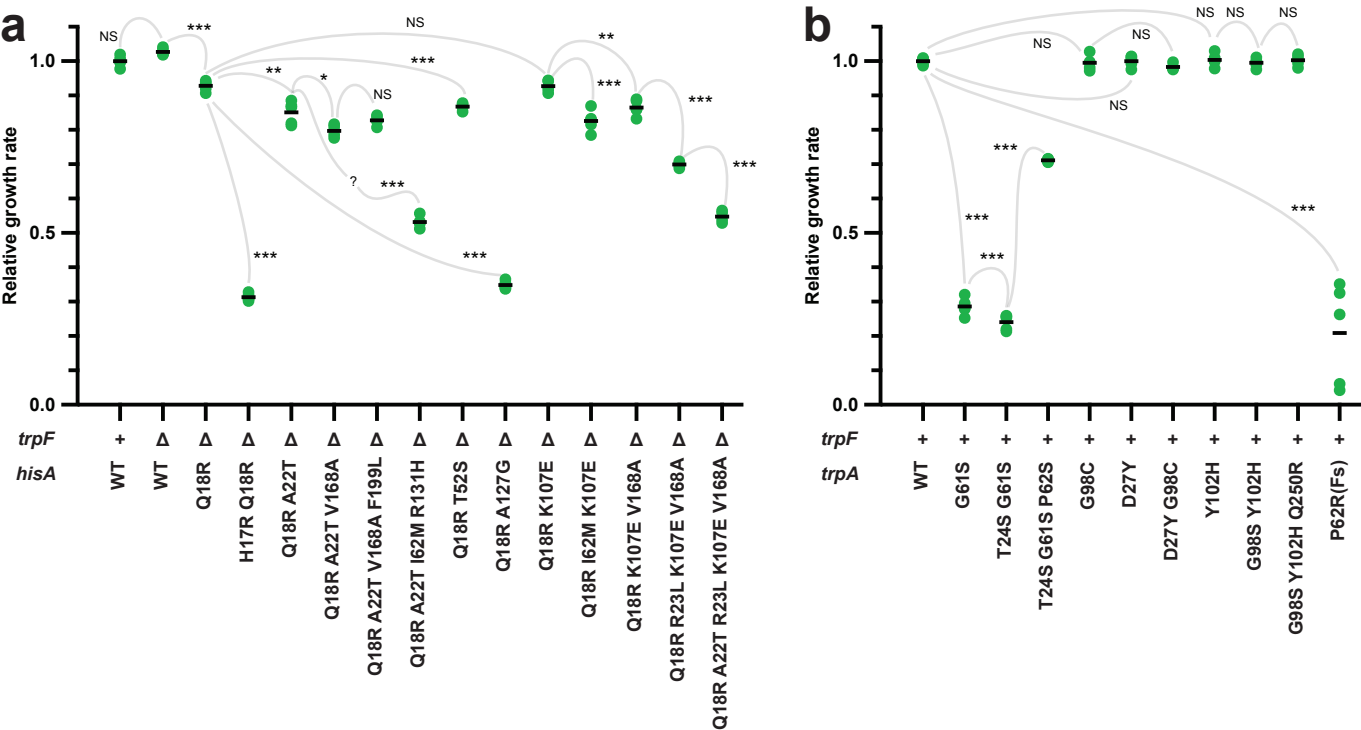
a
Relative growth rate
1.0
0.5
0.0
NS
***
NS
**
***
**
*
NS
?
***
***
***
***
***
***
trpF
hisA
+
WT
Δ
WT
Δ
Q18R
Δ
H17R Q18R
Δ
Q18R A22T
Δ
Q18R A22T V168A
Δ
Q18R A22T V168A F199L
Δ
Q18R A22T I62M R131H
Δ
Q18R T52S
Δ
Q18R A127G
Δ
Q18R K107E
Δ
Q18R I62M K107E
Δ
Q18R K107E V168A
Δ
Q18R R23L K107E V168A
Δ
Q18R A22T R23L K107E V168A
b
Relative growth rate
1.0
0.5
0.0
NS
NS
NS
NS
NS
NS
***
***
***
***
trpF
trpA
+
WT
+
G61S
+
T24S G61S
+
T24S G61S P62S
+
G98C
+
D27Y
+
D27Y G98C
+
Y102H
+
G98S Y102H
+
G98S Y102H Q250R
+
P62R(Fs)